

dimension; J , K , G and H are constant matrices of appropriate dimensions. For the system and the class of admissible controls described above, consider a mixed-attenuation problem state as below.

Problem 1 \mathcal{H}_∞ DIA control problem

Find an admissible control attenuating disturbances and initial state uncertainties in the way that, for given $N > 0$, z satisfies

$$\|z\|_2^2 < \|w\|_2^2 + x_0^T N^{-1} x_0 \quad (3)$$

for all $w \in L^2[0, \infty)$ and all $x_0 \in R^n$, s.t., $(w, x_0) \neq 0$.

Such an admissible control is called the **D**isturbance and **I**nitial state uncertainty **A**ttenuation (DIA) control.

In order to solve the \mathcal{H}_∞ DIA control problem, we require the so-called Riccati equation conditions:

(A1) There exists a $M > 0$ to the Riccati equation

$$\begin{aligned} & M(A - B_2(D_{12}^T D_{12})^{-1} D_{12}^T C_1) \\ & + (A - B_2(D_{12}^T D_{12})^{-1} D_{12}^T C_1)^T M \\ & - M(B_2(D_{12}^T D_{12})^{-1} B_2^T - B_1 B_1^T) M \\ & + C_1^T C_1 - C_1^T D_{12} (D_{12}^T D_{12})^{-1} D_{12}^T C_1 = 0 \end{aligned} \quad (4)$$

such that $A - B_2(D_{12}^T D_{12})^{-1} D_{12}^T C_1 - B_2(D_{12}^T D_{12})^{-1} B_2^T M + B_1 B_1^T M$ is stable.

(A2) There exists a $P > 0$ to the Riccati equation

$$\begin{aligned} & (A - B_1 D_{21}^T (D_{21} D_{21}^T)^{-1} C_2) P \\ & + P(A - B_1 D_{21}^T (D_{21} D_{21}^T)^{-1} C_2)^T \\ & - P(C_2^T (D_{21} D_{21}^T)^{-1} C_2 - C_1^T C_1) P \\ & + B_1 B_1^T - B_1 D_{21}^T (D_{21} D_{21}^T)^{-1} D_{21} B_1^T = 0 \end{aligned} \quad (5)$$

such that $A - B_1 D_{21}^T (D_{21} D_{21}^T)^{-1} C_2 - P C_2^T (D_{21} D_{21}^T)^{-1} C_2 + P C_1^T C_1$ is stable.

(A3) $\rho(PM) < 1$

where $\rho(X)$ denotes the spectral radius of matrix X , $\rho(X) = \max |\lambda_i(X)|$.

Then we can obtain the following result.

Theorem 1 [2]

Suppose that the conditions (A1), (A2) and (A3) are satisfied, then the central control is given by

$$\begin{aligned} u &= -(D_{12}^T D_{12})^{-1} (B_2^T M + D_{12}^T C_1) (I - PM)^{-1} \zeta \\ \dot{\zeta} &= A\zeta + B_2 u + P C_1^T (C_1 \zeta + D_{12} u) \\ & \quad + (P C_2^T + B_1 D_{21}^T) (D_{21} D_{21}^T)^{-1} (y - C_2 \zeta) \\ \zeta(0) &= 0 \end{aligned} \quad (6)$$

The central control (6) is the \mathcal{H}_∞ DIA control if and only if the condition (A4) is satisfied.

(A4) $Q + N^{-1} - P^{-1} > 0$,

where Q is the maximal solution of the Riccati equation

$$\begin{aligned} & Q(A - B_1 D_{21}^T (D_{21} D_{21}^T)^{-1} C_2 \\ & \quad + (B_1 B_1^T - B_1 D_{21}^T (D_{21} D_{21}^T)^{-1} D_{21} B_1^T) P^{-1}) \\ & \quad + (A - B_1 D_{21}^T (D_{21} D_{21}^T)^{-1} C_2 \\ & \quad + (B_1 B_1^T - B_1 D_{21}^T (D_{21} D_{21}^T)^{-1} D_{21} B_1^T) P^{-1})^T Q \\ & \quad - Q(B_1^T - D_{21}^T (D_{21} D_{21}^T)^{-1} (C_2 P + D_{21} B_1^T) L)^T \\ & \quad \times (B_1^T - D_{21}^T (D_{21} D_{21}^T)^{-1} (C_2 P + D_{21} B_1^T) L) Q \\ & = 0 \end{aligned} \quad (7)$$

with $L := (I - PM)^{-1}$.

SYSTEM DESCRIPTION AND MODELING

The experimental setup of the magnetic suspension system [8] is shown in FIG.1 and rotor coordinate is defined in FIG.2. The controlled plant is a 4-axis controlled type active magnetic bearing with symmetrical structure. The axial motion is not controlled actively. The electromagnets are located in the horizontal and the vertical direction of both sides of the rotor. Moreover, hall-device-type gap sensors are located in the both sides of the vertical and horizontal direction. The model parameter of the control plant is given in TABLE 1.

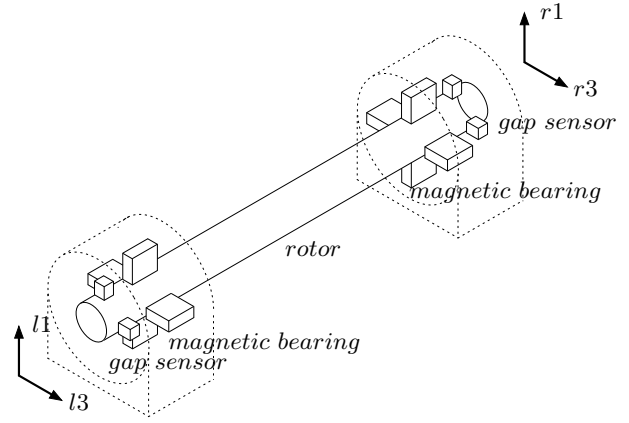


FIGURE 1: Active Magnetic Bearing

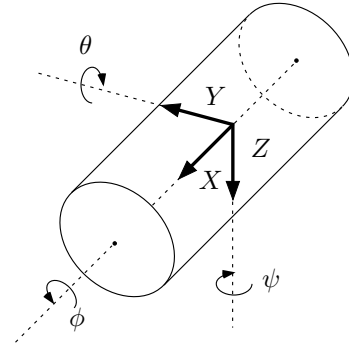


FIGURE 2: Rotor

In order to derive a nominal model of the system, the following assumptions are introduced[5].

- The rotor is rigid and has no unbalance.
- All electromagnets are identical.
- Attractive force of an electromagnet is in proportion to (electric current / gap length)².
- The resistance and the inductance of the electromagnet coil are constant and independent of the gap length.
- Small deviations from the equilibrium point are treated.

These assumptions are not strong and suitable around the steady state operation, but if the rotor spins at super-high speed, these assumption will be failed. Based on the

TABLE 1: MODEL PARAMETER

Parameter	Symbol	Value	Unit
Mass of the Rotor	m	0.248	kg
Length of the Rotor	L_R	0.269	m
Distance between Center of Mass and each Electromagnet	l_m	0.1105	m
Moment of Inertia about X	J_x	$5.05 \cdot 10^{-6}$	kgm ²
Moment of Inertia about Y	J_y	$1.59 \cdot 10^{-3}$	kgm ²
Steady Gap	G	0.4×10^{-3}	m
Coefficients of $f_j(t)$	k	2.8×10^{-7}	
Steady Current	I_{l1}, I_{r1}	0.1425	A
	I_{l3}, I_{r3}	0	A
Resistance	R	4	Ω
Inductance	L	8.8×10^{-4}	H
Steady Voltage	E_{l1}, E_{r1}	0.57	V
	E_{l3}, E_{r3}	0	V

above assumptions, the equation of the motion of the rotor in Y and Z directions in FIG.2 has been derived as follows[5].

$$m\ddot{y}_s = -f_{l3} - v_{ml3} - f_{r3} - v_{mr3} \quad (8)$$

$$m\ddot{z}_s = mg - f_{l1} - v_{ml1} - f_{r1} - v_{mr1} \quad (9)$$

$$J_y\ddot{\theta} = -J_x p\dot{\psi} + lm(f_{l1} + v_{ml1} - f_{r1} - v_{mr1}) \quad (10)$$

$$J_y\ddot{\psi} = -J_x p\dot{\theta} + lm(-f_{l3} - v_{ml3} + f_{r3} + v_{mr3}) \quad (11)$$

where $y_s(t)$ and $z_s(t)$ are displacements of Y direction and Z direction respectively; $\theta(t)$ and $\psi(t)$ are angles about Y direction and Z direction respectively; m is mass of the rotor; g is gravity; l_m is distance between center and electromagnet; J_x and J_y are Moments of Inertia about X axis and Y axis respectively; p is rotation rate of the rotor; f_j s are electromagnetic force; and v_{mj} s are exogenous disturbance. Here the subscript 'j' shows the each four directions: {l1, r1, l3, r3} in FIG.1.

The position variables y_s and z_s and the rotational variables θ and ψ can be transformed by using gap lengths: $\{g_{l1}, g_{r1}, g_{l3}, g_{r3}\}$ which are small deviations from the equilibrium point as follows.

$$y_s = -(g_{l3} + g_{r3})/2 \quad (12)$$

$$z_s = -(g_{l1} + g_{r1})/2 \quad (13)$$

$$\theta = (g_{l1} - g_{r1})/2l_m \quad (14)$$

$$\psi = (-g_{l3} + g_{r3})/2l_m \quad (15)$$

Attractive force of electromagnets is given by assumptions.

$$f_j = k \frac{(i_j + 0.5)^2}{(g_j - 0.0004)^2} - k \frac{(i_j - 0.5)^2}{(g_j + 0.0004)^2} \quad (16)$$

Next we linearize the electromagnetic force (16) around the operating point by the Taylor series expansions as

$$f_j = k \frac{(I_j + 0.5)^2 - (I_j - 0.5)^2}{1.6 \times 10^{-7}} + K_{xj}g_j + K_{ij}i_j \quad (17)$$

$$K_{xj} = -2k \left(\frac{(I_j + 0.5)^2}{(-4 \times 10^{-4})^3} + \frac{(I_j - 0.5)^2}{(4 \times 10^{-4})^3} \right)$$

$$K_{ij} = 2k \left(\frac{(I_j + 0.5)}{(-4 \times 10^{-4})^2} - \frac{(I_j - 0.5)}{(4 \times 10^{-4})^2} \right).$$

The electric circuit equations are given as followed.

$$L \frac{di_j(t)}{dt} + R(I_j + i_j(t)) = E_j + e_j(t) + v_{Lj}(t) \quad (18)$$

where $i_j(t)$ is a deviation from steady current; $e_j(t)$ is a deviation from steady voltage; v_{Lj} is noise.

The sensors provide the information for the gap lengths $g_j(t)$. Hence the measurement equations can be written as

$$y_j(t) = g_j(t) + w_j \quad (19)$$

where $w_j(t)$ represents the sensor noise as well as the model uncertainties.

Thus, summing up the above results (12)-(19), the state-space equations for the system are

$$\begin{bmatrix} \dot{x}_v \\ \dot{x}_h \end{bmatrix} = \begin{bmatrix} A_v & pA_{vh} \\ -pA_{vh} & A_h \end{bmatrix} \begin{bmatrix} x_v \\ x_h \end{bmatrix} + \begin{bmatrix} B_v & 0 \\ 0 & B_h \end{bmatrix} \begin{bmatrix} u_v \\ u_h \end{bmatrix} + \begin{bmatrix} D_v & 0 \\ 0 & D_h \end{bmatrix} \begin{bmatrix} v_v \\ v_h \end{bmatrix}$$

$$\begin{bmatrix} y_v \\ y_h \end{bmatrix} = \begin{bmatrix} C_v & 0 \\ 0 & C_h \end{bmatrix} \begin{bmatrix} x_v \\ x_h \end{bmatrix} + \begin{bmatrix} w_v \\ w_h \end{bmatrix} \quad (20)$$

$$x_v = [g_{l1} \ g_{r1} \ \dot{g}_{l1} \ \dot{g}_{r1} \ i_{l1} \ i_{r1}]^T$$

$$x_h = [g_{l3} \ g_{r3} \ \dot{g}_{l3} \ \dot{g}_{r3} \ i_{l3} \ i_{r3}]^T$$

$$u_v = [e_{l1} \ e_{r1}]^T, \quad u_h = [e_{l3} \ e_{r3}]^T$$

$$v_v = [v_{ml1} \ v_{mr1} \ v_{Ll1} \ v_{Lr1}]^T$$

$$v_h = [v_{ml3} \ v_{mr3} \ v_{Ll3} \ v_{Lr3}]^T$$

$$y_v = [y_{l1} \ y_{r1}]^T, \quad y_h = [y_{l3} \ y_{r3}]^T$$

$$w_v = [w_{l1} \ w_{r1}]^T, \quad w_h = [w_{l3} \ w_{r3}]^T$$

$$A_v := \begin{bmatrix} 0 & I_2 & 0 \\ K_{x1}A_1 & 0 & K_{i1}A_1 \\ 0 & 0 & -(R/L)I_2 \end{bmatrix}$$

$$A_h := \begin{bmatrix} 0 & I_2 & 0 \\ K_{x3}A_1 & 0 & K_{i3}A_1 \\ 0 & 0 & -(R/L)I_2 \end{bmatrix}$$

$$A_{vh} := \begin{bmatrix} 0 & 0 & 0 \\ 0 & A_2 & 0 \\ 0 & 0 & 0 \end{bmatrix}$$

$$A_1 := \begin{bmatrix} 1/m + l_m^2/J_y & 1/m - l_m^2/J_y \\ 1/m - l_m^2/J_y & 1/m + l_m^2/J_y \end{bmatrix}$$

$$A_2 := \begin{bmatrix} J_x/2J_y & -J_x/2J_y \\ -J_x/2J_y & J_x/2J_y \end{bmatrix}$$

$$\begin{aligned} B_v &= B_h := \begin{bmatrix} 0 \\ 0 \\ (1/L)I_2 \end{bmatrix} \\ C_v &= C_h := [I_2 \quad 0 \quad 0] \\ D_v &= D_h := \begin{bmatrix} 0 & 0 \\ A_1 & 0 \\ 0 & (1/L)I_2 \end{bmatrix} \end{aligned}$$

where $I_2 \in R^{2 \times 2}$ is unit matrix, and $K_{x1} = K_{xl1} = K_{xr1}$, $K_{x3} = K_{xl3} = K_{xr3}$, $K_{i1} = K_{il1} = K_{ir1}$, $K_{i3} = K_{il3} = K_{ir3}$ in (16), and p is the rotor speed. Here p is equal to 0 and we do not consider a rotation of the rotor in this paper.

The equation (20) can be also expressed simply as

$$\begin{aligned} \dot{x}_g &= A_g x_g + B_g u_g + D_g v_0 \\ y_g &= C_g x_g + w_0 \end{aligned} \quad (21)$$

where $x_g := [x_v^T \ x_h^T]^T$, $u_g := [u_v^T \ u_h^T]^T$, $v_0 := [v_v^T \ v_h^T]^T$, $w_0 = [w_v^T \ w_h^T]^T$ and A_g, B_g, C_g, D_g are constant matrices of appropriate dimensions.

CONTROL SYSTEM DESIGN

In this section, we design an \mathcal{H}_∞ DIA controller for the magnetic bearing system based on the derived state-space formula.

Let us construct a generalized plant for the magnetic bearing control system. First, consider the system disturbance v_0 . Since v_0 mainly acts on the plant in a low frequency range in practice, it is helpful to introduce a frequency weighting factor. Hence let v_0 be of the form

$$\begin{aligned} v_0 &= W_v(s)w_2 \quad (22) \\ W_v(s) &= \begin{bmatrix} I_2 & 0 \\ I_2 & 0 \\ 0 & I_2 \\ 0 & I_2 \end{bmatrix} W_{v0}(s) \\ W_{v0}(s) &= C_{v0}(sI_4 - A_{v0})^{-1} B_{v0} \end{aligned}$$

where $W_v(s)$ is a frequency weighting whose gain is relatively large in a low frequency range, and w_2 is a (1, 2) element of w . These values, as yet unspecified, can be regarded as free design parameters.

Consider the system disturbance w_0 for the output. The disturbance w_0 shows an uncertain influence caused via unmodeled dynamics, and define

$$\begin{aligned} w_0 &= W_w(s)w_1 \quad (23) \\ W_w(s) &= I_4 W_{w0}(s) \\ W_{w0}(s) &= C_{w0}(sI_4 - A_{w0})^{-1} B_{w0} \end{aligned}$$

where $W_w(s)$ is a frequency weighting function and w_1 is a (1, 1) element of w . Note that I_4 is unit matrix in $R^{4 \times 4}$.

The frequency functions W_v and W_w in (22) and (23) are rewritten as equations in (24) and (25).

$$\begin{aligned} \dot{x}_v &= A_v x_v + B_v w_2 \\ v_0 &= C_v x_v + D_v w_2 \end{aligned} \quad (24)$$

$$\begin{aligned} \dot{x}_w &= A_w x_w + B_w w_1 \\ w_0 &= C_w x_w + D_w w_1 \end{aligned} \quad (25)$$

where the state x_v and x_w are defined as

$$x_v := [x_{v1}^T \ x_{v2}^T \ x_{v3}^T \ x_{v4}^T]^T \quad x_w := [x_{w1}^T \ x_{w2}^T \ x_{w3}^T \ x_{w4}^T]^T$$

Next we consider the variables which we want to regulate. In this case, since our main concern is in the stabilization of the rotor, the gap and the corresponding velocity are chosen; i.e.,

$$z_g = F_g x_g, \quad (26)$$

$$F_g = \begin{bmatrix} I_2 & 0 & 0 & 0 & 0 & 0 \\ 0 & I_2 & 0 & 0 & 0 & 0 \\ 0 & 0 & 0 & I_2 & 0 & 0 \\ 0 & 0 & 0 & 0 & I_2 & 0 \end{bmatrix}$$

$$z_1 = \Theta z_g, \quad \Theta = \text{diag} [\theta_1 \quad \theta_2 \quad \theta_1 \quad \theta_2] \quad (27)$$

where Θ is a weighting matrix on the regulated variables z_g , and z_1 is a (1, 1) element of z . This value Θ , as yet unspecified, are also free design parameters.

Furthermore the control input u_g should be also regulated, and we define

$$z_2 = \rho u_g \quad (28)$$

where ρ is a weighting scalar, and z_2 is a (1, 2) element of z . Finally, let $x := [x_g^T \ x_v^T \ x_w^T]^T$, where x_v denotes the state of the function $W_v(s)$, x_w denotes the state of the function $W_w(s)$, and $w := [w_1^T \ w_2^T]^T$, $z := [z_1^T \ z_2^T]^T$, then we can construct the generalized plant as follows.

$$\begin{aligned} \dot{x} &= Ax + B_1 w + B_2 u \\ z &= C_1 x + D_{12} u \\ y &= C_2 x + D_{21} w \end{aligned} \quad (29)$$

Since the disturbances w represent the various model uncertainties, the effects of these disturbances on the error vector z should be reduced.

Next our control problem setup is defined as;

Control problem Find an admissible controller $K(s)$ that attenuates disturbances and initial state uncertainties to achieve the \mathcal{H}_∞ DIA condition in (3) for generalized plant (29).

After some iteration in MATLAB environment, design parameters are chosen as follows;

$$\begin{aligned} W_{v0}(s) &= \frac{40000}{s + 0.1} \\ W_{w0}(s) &= \frac{1.1s^3 + 1.4 \cdot 10^4 s^2 + 7.3 \cdot 10^7 s + 3.5 \cdot 10^{11}}{0.2s^3 + 1.1 \cdot 10^4 s^2 + 5.1 \cdot 10^6 s + 2.7 \cdot 10^{11}} \\ \Theta &= \text{diag} [\theta_{v1} \quad \theta_{v2} \quad \theta_{h1} \quad \theta_{h2}] \\ \theta_{v1} &= \text{diag} [0.4 \quad 0.4], \\ \theta_{h1} &= \text{diag} [0.5 \quad 0.5] \\ \theta_{v2} &= \theta_{h2} = \text{diag} [0.0005 \quad 0.0005] \\ \rho &= 8.0 \cdot 10^{-7} I_4 \end{aligned}$$

Direct calculations yield the 24-order \mathcal{H}_∞ DIA central controller K_{DIA} and its frequency response is shown in FIG.3.

The maximum value of the weighting matrix N in the \mathcal{H}_∞ DIA condition (3) is given by

$$N = 3.3176 \cdot 10^{-6} \cdot I_{24}. \quad (30)$$

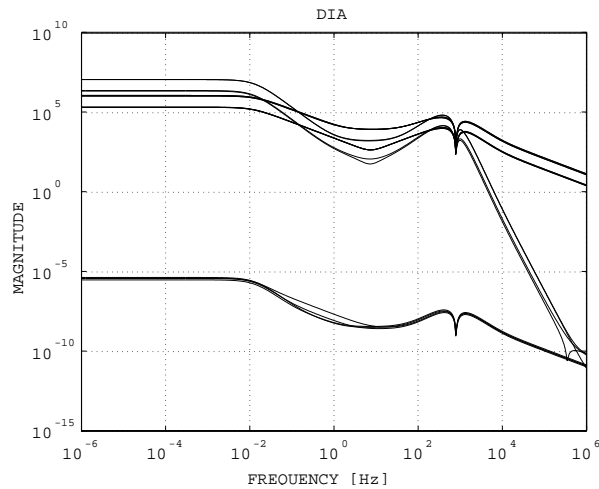


FIGURE 3: Frequency Responses of \mathcal{H}_∞ DIA Controllers

EVALUATION BY EXPERIMENTS

We conducted control experiments to evaluate properties of the designed \mathcal{H}_∞ DIA controller compared with an integral-type Optimal State Feedback Control with the minimal order observer and a notch filter. We define this controller as “LQ Controller”.

The notch filter has a notch at 2000[Hz] and its transfer function is as follows.

$$\frac{s^2 + 1.5791 \times 10^8}{s^2 + 12566s + 1.5791 \times 10^8} \quad (31)$$

The objective of this experimental comparison is to evaluate control performance for transient property, robust performance and initial response for uncertain initial state. The experimental results are shown in FIGs. 4-9.

1) Step Responses

Step responses for a reference signal are shown in FIG.4 and FIG.7, where the step size is 0.05[mm] and the steady-state gap is 0.4[mm]. Compared with \mathcal{H}_∞ DIA control, LQ control shows a quick response without any overshoot because LQ control utilizes full state information.

2) Disturbance Responses

Disturbance responses for a step-type disturbance signal with/without model parameter perturbation are shown in FIG.5 and FIG.8. A 60[g] weight is attached to the center of the rotor as a model perturbation and a step-type force disturbance is added to $-l1$ and $-r1$ directions in FIG.1, where the magnitude of the disturbance is 1/6 steady-state vertical attractive force.

\mathcal{H}_∞ DIA controller shows good disturbance responses and also good robust performance for step-type disturbance and model perturbation.

3) Initial Responses

In FIGs.6 and 9, initial responses of two controllers are shown respectively. The initial state is chosen that the

rotor is touched down. Four gap lengths are shown in these figures and the \mathcal{H}_∞ DIA controller shows better initial performance.

Finally, compared with LQ control, we can see that \mathcal{H}_∞ DIA control has a good robust performance and transient response except for nominal step response from FIGs.4-9.

CONCLUSION

This paper dealt with an application of \mathcal{H}_∞ control attenuating initial-state uncertainties to the magnetic bearing and examined the \mathcal{H}_∞ DIA control problem.

First we derived a mathematical model of magnetic bearing systems considering rotor dynamics and nonlinearities of magnetic force. Then we set the generalized plant which contains design parameter for uncertainty and control performance.

Finally, several experimental results of step responses and disturbance responses with model perturbation and initial responses showed that the proposed \mathcal{H}_∞ DIA robust control approach is effective for a mixed disturbance and an initial-state uncertainty attenuation and for improving transient response and robust performance.

Future work is an evaluation of the proposed \mathcal{H}_∞ DIA control via rotational experiments.

REFERENCES

- [1] T. Sugie and Y. Tanai, “ H_2/H_∞ Suboptimal Controller Design of Magnetic Levitation Systems(in Japanese),” *Trans. SICE*, vol. 30, no. 10, pp. 1202 - 1208, 1994.
- [2] T. Namerikawa, M. Fujita, R.S. Smith and K. Uchida, “On the \mathcal{H}_∞ Control System Design Attenuating Initial State Uncertainties,” *Trans. of SICE*, vol.40, no.3. pp.307-314, 2004.
- [3] T. Namerikawa and M. Fujita, “ \mathcal{H}_∞ Control System Design of the Magnetic Suspension System Considering Initial State Uncertainties,” *IEEJ Trans. EIS*, vol.123, no.6, pp.1094-1100, 2003.
- [4] G. R. Duan and D. Howe, “Robust Magnetic Bearing Control via Eigenstructure Assignment Dynamical Compensation,” *IEEE Trans. on CST*, vol. 11, no. 2, pp. 204-215, 2003.
- [5] F. Matsumura, T. Namerikawa, K. Hagiwara and M. Fujita, “Application of Gain Scheduled \mathcal{H}_∞ Robust Controllers to a Magnetic Bearing,” *IEEE Trans. on CST*, vol. 4, no. 5, pp. 484-493, 1996.
- [6] J. H. Lee, P. E. Allaire, G. Tao, J. A. Decker and X. Zhang, “Experimental study of sliding mode control for a benchmark magnetic bearing system and artificial heart pump suspension,” *IEEE Trans. on CST*, vol. 11, no. 1, pp. 128-138, 2003.
- [7] K. Nonami and T. Ito, “ μ Synthesis of Flexible Rotor-Magnetic Bearing Systems,” *IEEE Trans. on CST*, vol. 4, no. 5, pp. 503-512, 1996.
- [8] Magnetic Moments, LLC, *MBC 500 Magnetic Bearing System Operation Instructions*, 2002.

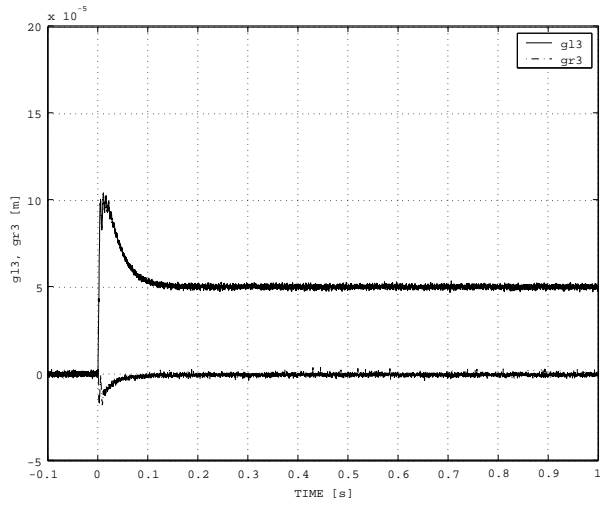


FIGURE 4: Step Response of \mathcal{H}_∞ DIA Controller

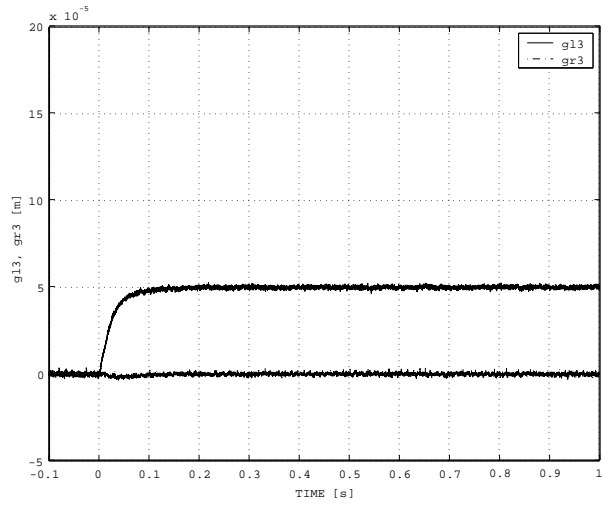


FIGURE 7: Step Response of LQ Controller

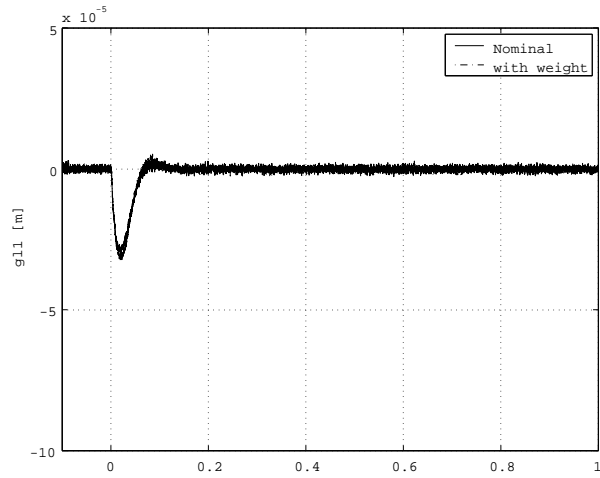


FIGURE 5: Disturbance Response of \mathcal{H}_∞ DIA Controller with/without perturbation

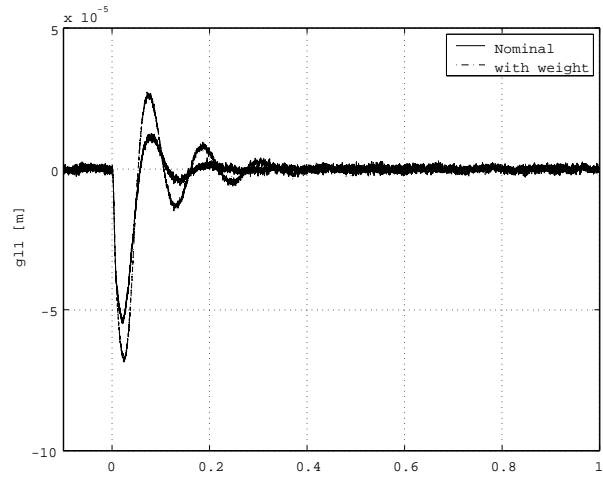


FIGURE 8: Disturbance Response of LQ Controller with/without perturbation

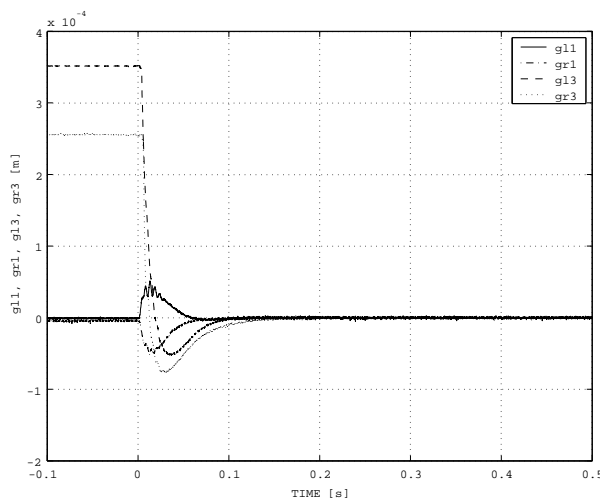


FIGURE 6: Initial Response of \mathcal{H}_∞ DIA Controller

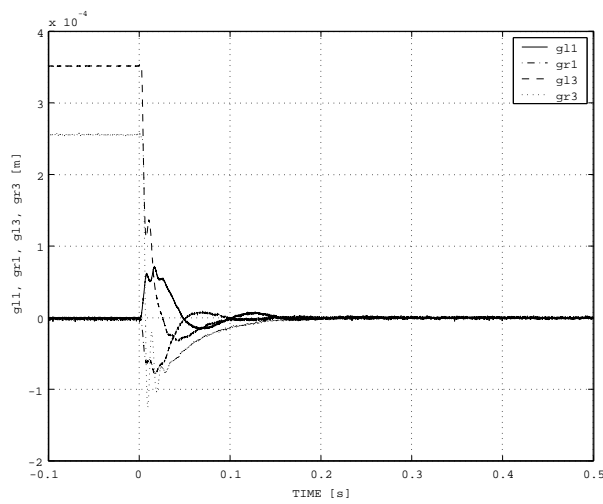


FIGURE 9: Initial Response of LQ Controller